A 300 parsec long jet-inflated bubble around a powerful microquasar in the galaxy NGC 7793

Manfred W. Pakull[1], Roberto Soria[2], Christian Motch[1],

[1] *University of Strasbourg, CNRS UMR 7550, Observatoire Astronomique, 11 rue de l'Université, F67000 Strasbourg, F*

[2] *MSSL, University College London, Holmbury St Mary, Surrey RH5 6NT, UK*

Black hole accretion states near or above the limiting Eddington luminosity, at which radiation pressure overcomes gravitational forces, are still poorly known because of the rarity of such sources in today's Universe. Ultraluminous X-ray sources (ULXs)[1] are the most luminous class of non-nuclear black holes (Lx $\sim 10^{40}$ erg s^{-1}), and are often associated with shock-ionized nebulae[2,3] but with no evidence of collimated jets; microquasars with steady jets are much less luminous. Here we report our discovery that the large nebula S26[4] in the nearby galaxy NGC 7793 is powered by a black hole with a pair of collimated jets. S26 is similar to the radio nebula W50 around the famous Galactic source SS433[5], but twice as large and many times more powerful. We determine a mechanical power $\sim$ a few 10^{40} erg s^{-1} from the optical line flux, the expansion velocity and the size of the cocoon. Thus the jets appear much more energetic than the X-ray emission from the core. S26 has the textbook structure of an FRII-type active galaxy: X-ray and optical core; X-ray hot spots; radio lobes[9] and X-ray cocoon. S26 is a microquasar where most of the jet power is dissipated in the form of thermal particles rather than relativistic electrons.

The very large, shock-ionized nebulae (ULX bubbles[6]), with characteristic sizes ~ 100–500 pc and ages $\sim$ a few 10^5 yr are much larger and more energetic than normal supernova remnants (SNRs). But X-ray luminous sources may be only a subset of non-nuclear black holes at very high mass accretion rates. We proposed[7] that ionized bubbles might also be found associated with black holes that appear X-ray faint, either because their radiative emission is collimated away from our line of sight, or because they are transients and currently in a low/off accretion state, or because they channel most of their accretion power into a jet even at near-Eddington mass accretion rates.

Using the *Chandra Data Archive* we searched for such systems among unusually large SNRs in nearby galaxies and discovered a spectacular example in the Sculptor galaxy NGC 7793 (distance of 3.9 Mpc[8]). The optical/radio nebula S26[4,9] has a size of $\approx 300 \times 150$ pc and was originally classified as a supernova remnant candidate; the high [S II] $\lambda 6716, 32/\mathrm{H}\alpha$ flux ratio indicates the presence of shock-ionized gas. A faint X-ray source[10] was known to be associated with S26, but it was unresolved in the *ROSAT* observation. The X-ray emission is resolved into three point-like sources that are perfectly aligned and match the extent of the major axis of the optical nebula (Fig. 1). We interpret those sources as the core (at the X-ray binary position) and the hot spots (where the jet interacts with the ambient medium). The core appears harder with an intrinsic 0.3–10 keV power-law luminosity $L_{0.3-10} \approx 7 \times 10^{36}$ erg s^{-1}, while the hot spots have a softer spectrum and can be fitted by optically-thin thermal plasma emission (Fig. 2) with a combined intrinsic luminosity $L_{0.3-10} \approx 1.8 \times 10^{37}$ erg s^{-1}. Faint, even softer diffuse X-ray emission pervades much of the extent of the optical bubble. The morphology strikingly resembles that of an FRII-type powerful active galaxy, displaying X-ray and radio hot spots (e.g., Cyg A[11]). The optical radial velocity of S26 agrees with that of other nearby nebulæ in NGC 7793 (cf. Fig. 4), effectively ruling out a chance superposition of a background AGN.

Optical narrow-band He II$\lambda 4686$ and nearby continuum imaging observations (Fig. 3) reveal that NGC 7793 emits significant amounts of He^{++} $\rightarrow$ He^{+} $\lambda 4686$ recombination photons with approximately the same spatial distribution as Hα emission. This implies that either the central star is both extremely luminous and sufficiently hot (i.e. $T_{\rm eff} \geq 80\,000 K$) to be able to photoionize the large He III region, or alternatively that the gas has been ionized by a very fast shock wave. We will show below that the second possibility is realized in S26.

The images show (Fig. 3, left panel) that the optical counterpart of the X-ray core is a blue stellar object with an absolute magnitude $\mathrm{M_B} \approx -5$ mag. Moreover, we detect an excess of stellar $\lambda 4686$ emission (Fig. 3, right panel) with an equivalent width EW ≈ 30 Å. This is similar to what we expect from an early-type Wolf-Rayet star (type WNE). As an aside, such type of evolved star is the mass donor in IC 10 X-1[12], the most massive stellar BH presently known[13], which is also embedded in a large synchrotron bubble. This bubble and S26 have sometimes been attributed to a hypothetical hypernova event[14,9,15].

We have now obtained key optical spectroscopic observations that allow us to directly measure the expansion (shock) velocity of S26 and thus estimate the energetics of the system. From the half-width at zero-intensity of the main emission lines, we estimate that the gas is supersonically expanding with a maximum velocity envelope $v_{\rm exp} \approx 250$ km s^{-1} (Fig. 4). An independent estimate of the shock velocity can be derived from the relative strength of the He II $\lambda 4686$ line with respect to the H I Balmer emission. We measure a flux ratio $I_{\lambda 4686}/I_{\mathrm{H}\beta} \approx 0.09$–$0.12$. From a standard library of radiative shocks[16], we find that this diagnostic line ratio implies $v_{\rm shock} \approx 275 \pm 25$ km s^{-1}, if precursor emission is taken into account, in remarkable agreement with the kinematic velocity estimate. Futhermore, the diagnostic [O III] forbidden line ratio $I_{\lambda 5007}/I_{\lambda 4363}$ corresponds to an electron temperature $T_e \approx 27,000$ K, typical of shock-ionized gas, and inconsistent with photo-ionization, which would yield electron temperatures closer to $\approx 10,000$ K.

We are now in a position to reliably estimate the energetics of this jet-inflated bubble. To this end we use the well-known self-similar expansion law[17,18] as a function of time, t, for wind-driven stellar bubbles and jet-driven radio lobes: $R \simeq 0.76(Q_{\rm jet}/\rho_0)^{1/5} \times t^{3/5}$, where $Q_{\rm jet}$ is the long-term-averaged jet power, R is the (mean) radius of the bubble expanding with velocity $v_{\rm exp} = dR/dt$ into the interstellar medium (ISM) with an assumed constant ISM density. The first conclusion we can draw is that the characteristic age of the bubble is $t = \frac{3}{5}R/v_{\rm exp} \approx 2 \times 10^5$ yr. The even more interesting jet power $Q_{\rm jet}$ can be derived from standard bubble theory[17] which implies that a fraction 22/77 of the jet power $Q_{\rm jet}$ is emitted by a fully radiative shock expanding into the IS medium. Furthermore, radiative shock models[19] predict that for an observed $v_{\rm shock} \approx 275$ km s^{-1}, 0.77% of the radiated energy appears as Hβ photons if we include the effect of a radiative precursor. This implies that the Hβ luminosity ($\approx 1.0 \times 10^{38}$ erg s^{-1}; cf. Fig. 1) can be used to directly estimate the jet power. This implies $Q_{\rm jet} \approx 5 \times 10^{40}$ erg s^{-1} which is a remarkably high power for a Galactic-type accreting source. Using the formalism outlined in ref.[6,19] we find a hydrogen particle density of the ISM into which S26 expands to be $n \approx 0.7$ cm^{-3}. The mechanical energy of the swept-up shell is $1/2 M v_{\rm exp}^2 = (15/77)\, Q_{\rm jet}\, t$ (see ref. [17]) where $M = 4\pi/3 \times 1.38\, m_{\rm p}\, n\, R^3$.

This yields, again, the same $Q_{\rm jet}$ as derived before.

The long-term-averaged jet power observed in S26 is an order of magnitude higher than what is estimated for the already very powerful, mildly relativistic jets from the Galactic microquasar SS433[5,20]. Perhaps more importantly, we find that $Q_{\rm jet}$ exceeds the apparent X-ray luminosity of the core by about a factor of 10^4. A similar dominance of mechanical power over (observed) radiative power in SS433 has traditionally been ascribed to absorption of X-rays along our line-of-sight (source seen along the plane of the accretion disk[21]). The discovery of a second, even more extreme X-ray-faint jet source, with a mechanical power well above the Eddington limit for a stellar-mass black hole, suggests that there may be accretion modes which channel most of the available power into jets rather than photons, even at extremely high mass accretion rates[22].

With its extraordinarily rich, interconnected structure of optical, X-ray and radio emission, S26 provides new observational tests for our physical understanding of accretion-powered astrophysical sources and of their energy transfer into the surrounding gas. S26 is the missing link between the similarly large and energetic ULX bubbles (in which there is yet no direct evidence of collimated jets) and the Galactic jet source SS433 with its comparatively smaller, fainter nebula W50. It is also the first true non-nuclear analogue of powerful FRII active galaxies with their persistent radio lobes.

The jet power we have derived for S26 is orders of magnitude larger than the value one would derive from the radio luminosity of the nebula, using the popular relations for microquasar lobe dynamics[23]. The reason for this discrepancy is the underlying assumption that most of the power is converted into non-thermal relativistic particles (including the radiating leptons) and into magnetic fields. These in turn are thought to provide the pressure that drives the expansion of the microquasar lobes. But much more thermal energy may be stored in non-relativistic protons and nuclei. Much higher kinetic jet power than previously thought, possibly even surpassing the Eddington luminosity, has recently been advocated for several powerful FRII-type active galaxies[24]; this suggests that most of the energy in their cocoons is carried by thermal particles, as it appears to be the case for S26.

1. Ward, M. Luminous X-ray sources in spiral and star-forming galaxies *Phil. Trans. R. Soc. Lond. A.* **360**, 1991-2003 (2002)

2. Pakull, M.W. & Mirioni, L. Optical Counterparts of Ultraluminous X-ray Sources, arXiv Astrophysics e-prints, *0202488* (2002)

3. Pakull, M.W. & Mirioni, L. Bubble Nebulæ around Ultraluminous X-ray Sources *ReV. Mex. AA. Ser. Conf.* **15**, 197-199 (2003)

4. Blair, W.P. & Long, K. S. Identification of supernova remnants in the Sculptor galaxies NGC 300 and NGC 7793 *Astrophys. J. Supp. Series* **108** 261-277 (1997)

5. Fabrika, S. The Jets and the Supercritical Accretion Disk in SS433 *Astrophys. Space. Phys. Rev.* **12**, 1-153 (2004)

6. Pakull, M. W., Grisé, F., & Motch, C. Ultraluminous X-ray sources: Bubbles and optical counterparts, IAU Symposium, Vol. **230**, Populations of High Energy Sources in Galaxies, ed.

E. J. A. Meurs & G. Fabbiano, 293-297 (2006)

7. Pakull, M.W. & Grisé, F. Ultraluminous X-ray Sources: Beambags and Optical Counterparts *AIP Conf. Proc.* **1010**, AIP, New York, 303-307 (2008)

8. Karachentsev, I. D., Grebel, E. K., Sharina, M. E., Dolphin, A. E., Geisler, D., Guhathakurta, P., Hodge, P. W., Karachentseva, V. E., Sarajedini, A. Seitzer, P. Distances to nearby galaxies in Sculptor *Astron. Astrophys.* **404**, 93-111 (2003)

9. Pannuti, T.G., Duric, N., Lacey, C.K., Ferguson, A.M.N., Magnor, M.A. & Menelowitz, C. An X-ray, Optical and radio Search for Supernova Remnants in the nearby Sculptor Group Sd Galaxy NGC 7793 *Astrophys. J.* **565**, 966-981 (2002)

10. Read, A.M., Pietsch, W. ROSAT observations of the Sculptor Galaxy NGC 7793 *Astron. Astrophys.* **341**, 8-22 (1999)

11. Wilson, A.S., Smith, D.A., Young, A.J. The cavity of Cyg A *Astrophys. J. Lett.* **644**, L9-L12 (2006)

12. Clark, J.S., Crowther, P.A. On the Wolf-Rayet Counterpart to IC 10 X-1 *Astron. Astrophys.* **414**, L45-L48 (2004)

13. Silverman, J.M., Filippenko, A.V. On IC 10X-1, the most massive known stellar-mass black hole *Astrophys. J. LetChandra/ACs26final.texIS-S X-ray spectrat.* **678**, L17-L20 (2009)

14. Lozinskaya, T.A. & Moiseev, A.V. A synchrotron Superbubble in the IC 10 Galaxy: a hypernova Remnant ? *Mon. Not. Roy. Astron. Soc.* **381**, L26-L29 (2007)

15. Asvarov, A.I. Radio emission from shell-type supernova remnants *Astron. Astrophys.* **459**, 519-533 (2006)

16. Allen, M.G., Groves, B.A., Dopita, M.A., Sutherland, R.S., Kewley, L.J. The MAPPINGS III Library of Fast Radiative Shock Models *Astrophys. J. Suppl. Ser.* **178**, 20-55 (2008)

17. Weaver, R., McCray, R., Castor, J., Shapiro, P., Moore, R. Interstellar Bubbles. II - Structure and evolution *Astrophys. J.* **218**, 377-395 (1977)

18. Kaiser, C. R. & Alexander, P. A self-similar model for extragalactic radio sources. *Mon. Not. Roy. Astron. Soc.* **286**, 215-222 (1997)

19. Dopita, M.A., Sutherland, R.S. Spectral Signatures of Fast Shocks. I. Low-Density Model Grid *Astrophys. J. Supp. Series* **102**, 161-188 (1996)

20. Begelman, M.C., Hatchett, S.P., McKee, C.F., Sarazin, C.L., Aarons, J. Beam models for SS433 *Astrophys. J.* **238**,722-730 (1980)

21. Begelman, M.C., King, A.R., Pringle, J.E. The Nature of SS 433 and the Ultraluminous X-ray Sources *Mon. Not. Roy. Astron. Soc.* **370**, 399-404 (2006)

22. Bogovalov, S.V., Kel’ner, S.R. Dissipationless Disk Accretion *Astron. Reports* **49**, 57-70 (2005)

23. Heinz, S. Radio lobe dynamics and the environment of microquasars *Astron. Astrophysics* **388**, L40-L43 (2002)

24. Ito, H., Kino, M., Nozomu, K., Isobe, N., Shoishi, Y. The Estimate of Kinetic Power of Jets in FR II Radio Galaxies: Existence of Invisible Components ? *Astrophys. J.* **685**, 828-838 (2008)

25. Kennicutt, R. C., Jr., Lee, J. C., Funes, S. J., José G., Sakai, S., & Akiyama, S. An HI Imaging Survey of Galaxies in the Local 11 Mpc Volume *Astrophys. J. Suppl* **178**, 247-279 (2008)

26. Dopita, M. A., Sutherland, R. S. Astrophysics of the diffuse universe, Berlin, New York: Springer, Astronomy and astrophysics library, (2003)

27. Raymond, J.C., Hester, J.J., Cox, D., Blair, W.P., Fesen, R.A., Gull, T.R. Spatial and Spectral Interpretation of a Bright Filament in the Cygnus Loop *Astrophys. J.* **324**, 869-892 (1988)

Author contributions: The authors have contributed equally to this Letter.

Competing interest statement: The authors declare that they have no competing financial interest.

Author information: Correspondence and requests for materials should be addressed to MWP manfred.pakull@astro.unistra.fr) or to R.S. (rsoria@physics.usyd.edu.au)

Acknowledgements: Based on observations made with ESO telescopes at the Paranal Observatory under program 084.D-0881 (Pakull). This research has made use of the ESO/ST-ECF Science Archive facility, which is a joint collaboration of the ESO and Space Telescope European Coordonating Facility, and of data obtained from the *Chandra Data Archive*, and software provided by the *Chandra X-ray center (CXC)* *received:* 22 01 2010; *accepted:* 05 05 2010

Figure 1: Optical/X-ray image of the 300 pc diameter jet-inflated bubble S26 in the galaxy NGC 7793. The contours denote the continuum-subtracted Hα emission which is plotted over a true-colour *Chandra*/ACIS-S image (ObsId=3954; P.I.: T.G. Pannuti). The projected distance between the X-ray hot spots is ≈ 15 arcsec ≈ 290 pc at the distance of NGC 7793. The *Chandra* exposure time was ≈ 50 ks. The X-ray colours are: red $= 0.3$–1 keV; green $= 1$–2 keV; blue $= 2$–8 keV. All three colour images in the X-ray band were lightly smoothed with a 1 arcsec Gaussian core. The continuum subtracted Hα image was taken with the CTIO 1.5-m telescope in 2001 (exposure time 600 sec, under 1.2 arcsec FWHM seeing condition) for the Spitzer Infrared Nearby Galaxy Survey (SINGS)[25] and downloaded through the NASA/IPAC Extragalctic Database (NED). We used matching point-like sources in the full field of NGC 7793 to improve the relative astrometry of the Hα and X-ray images. Note the relatively softer X-ray colour of the hot spots, compared with the blue point-like core; even softer, diffuse X-ray emission is detected over the whole nebula. The intrinsic X-ray luminosity of the Southern hot spot is twice as high as the luminosity of the Northern hot spot; this is similar to the higher Hα intensity in that region. There is no Hα point-like source or enhanced emission at the position of the X-ray core. The other source of Hα emission a few arcsec to the East of S26 is an unrelated H II region. Scaling from the total Hα luminosity of NGC 7793[25], and assuming a Hα/Hβ Balmer decrement ~ 3.0, we determined an Hβ luminosity of $\approx 1.0 \times 10^{38}$ erg s^{-1}.

Figure 2: ***Chandra*****/ACIS-S spectra of the triple X-ray source in S26**. Emission from the two hot spots (added together) and of the central source of S26 are shown with red and blue data points, respectively. The data were extracted from the Chandra archive and analysed with the standard software packages CIAO and XSPEC. We found that the central source has a hard spectrum (photon index $\Gamma = 1.4 \pm 0.5$) and an intrinsic 0.3–10 keV luminosity $L_{0.3-10} \approx 7 \times 10^{36}$ erg s^{-1}, *i.e.*, much less than the Eddington limit of a neutron star or a stellar-mass black hole. The emission from the hot spots is significantly softer and is well fitted by a two-component thermal plasma model with $kT_1 = 0.26^{+0.05}_{-0.08}$ keV, $kT_2 = 0.96^{+0.31}_{-0.17}$ keV (contributing roughly equally to the total flux), and no significant absorption above the Galactic line-of-sight column density $N_{\rm H} = 1.2 \times 10^{20}$ cm^{-2}. We derive intrinsic luminosities $L_{0.3-10} \approx 1.2 \times 10^{37}$ erg s^{-1} and $L_{0.3-10} \approx 0.6 \times 10^{37}$ erg s^{-1} for the Southern and Northern hot spot, respectively. The particle density n_X of the X-ray emitting, shocked thermal plasma (assumed to have solar abundance) can be estimated as $n_X \approx 2 \times \theta^{-3/2}$ cm^{-3}, where θ is the diameter of the emitting hot spots in units of arcsec. A characteristic hot spot size ≈ 1 arcsec is suggested by the marginally-resolved *Chandra* image. This gives a mass of the X-ray emitting gas of $\approx 500 \times \theta^{-3/2}$ M$_\odot$, more than can be supplied by a donor star orbiting the black hole. It probably represents a mix between the very hot but dilute jet gas that has passed through the reverse (Mach) shock and the much denser material behind the foreward (bow) shock, which is advancing into the interstellar medium. Alternatively, a very steep power-law spectrum with $\Gamma = 5.7 \pm 1.4$ and $N_{\rm H} = (4 \pm 2) \times 10^{21}$ cm^{-2} cannot presently be excluded, but appears to contradict both the low observed optical reddening[4] and the expected slope for a synchrotron component extending from the radio to the X-ray bands.

Figure 3: The stellar and high-excitation nebular content of S26. Left panel: optical-continuum greyscale image of S26, taken with the FORS1 instrument on the ESO Very Large Telescope (VLT) in 2002 and downloaded from the public archive. The narrow-band filter used for this image was centred at 5105 Å, with a full-width half-maximum of 61 Å (exposure time 1600 s under 1.0-1.5 arcsec FWHM seeing conditions). The size and orientation of the image are as in Fig. 1. The positions of the X-ray core and hot spots have been overplotted as red circles with 0.7-arcsec radius. Note the relative brightness of the optical counterpart to the X-ray core; we estimate $B \approx 23$ mag, corresponding to $M_B \approx -5$ mag. Right panel: continuum-subtracted greyscale FORS1 image in the He II $\lambda 4686$ emission (narrow-band filter centred at 4684 Å, with a full-width half-maximum of 65 Å; exposure time and seeing conditions were the same as for the 5105 Å image). The image was smoothed with a 0.6 arcsec Gaussian core, to highlight the extended nebular line emission. The observed flux ratio between He II $\lambda 4686$ and the H I Balmer lines suggests shock ionization with $v_s \approx 275$ km s^{-1}. Note also the point-like He II $\lambda 4686$ emission from the core, for which we estimate an equivalent width ≈ 30 Å. The green lines show position and width of the slit used to acquire the spectrum shown in Fig. 4.

Figure 4: Spectrum of Doppler-broadened emission lines of S26 indicating an expansion velocity of 250 km/s. Part of a medium resolution (~ 0.7 Å FWHM) long-slit ESO VLT FORS2 spectrum (taken in October 2009) covering $\lambda\lambda$3600-7200Å, with the slit running across the eastern body of S26 as shown in Fig. 3. The exposure times for the red and blue settings were 2200 s under good seeing conditions (FWHM=0.7-0.8 arcsec). The reduced spectra were analysed using ESO-MIDAS routines. The dispersion is along the horizontal axis with increasing wavelengths towards the right. In the vertical (spatial) direction, one pixel corresponds to ≈ 0.2 arcsec; the total extent of S26 is ≈ 10 arcsec along the slit. Narrow, constant intensity, vertical emission lines are due to spectroscopically unresolved atmospheric O and OH night-glow; the most prominent emission lines from S26 are, from left to right, [N II]λ6548, H_α, and [N II]λ6584. The 'bulged' appearance, mostly visible in the intense H_α emission, reflects the amazing kinematics of the emitting material in S26. The small extent in wavelength at the lower and upper nebular boundaries reflects the small velocities of the emitting gas along our line-of-sight (i.e. mostly perpendicular motion). The central part of the line covers the whole range of radial velocities across the nebula, which we assign to expansive motion from zero up to 250 km s^{-1} around a central velocity which is close to the apparent radial velocity in that part of NGC 7793. The density of the ISM ($n \approx 0.7$ cm^{-3}; see text) is sufficiently high to assure that the cooling time behind the shock $\tau \approx 200\frac{v_{100}^{4.4}}{Zn}$ yrs[26] (where $v_{100} = v_{\mathrm{s}}/(100\mathrm{km\,s}^{-1})$ and Z the metallicity relative to the solar value) is smaller than the age of the bubble. Therefore, the cooling/recombination zone behind the shock is largely complete, *i.e.*, the shock is largely radiative[27], in agreement with the presence of relatively strong low-ionisation or neutral species. One such diagnostic species is [O I], which emits the $\lambda 6300$ line[4]

with $I_{\lambda 6300}/I_{\mathrm{H}\beta} \approx 0.63$.

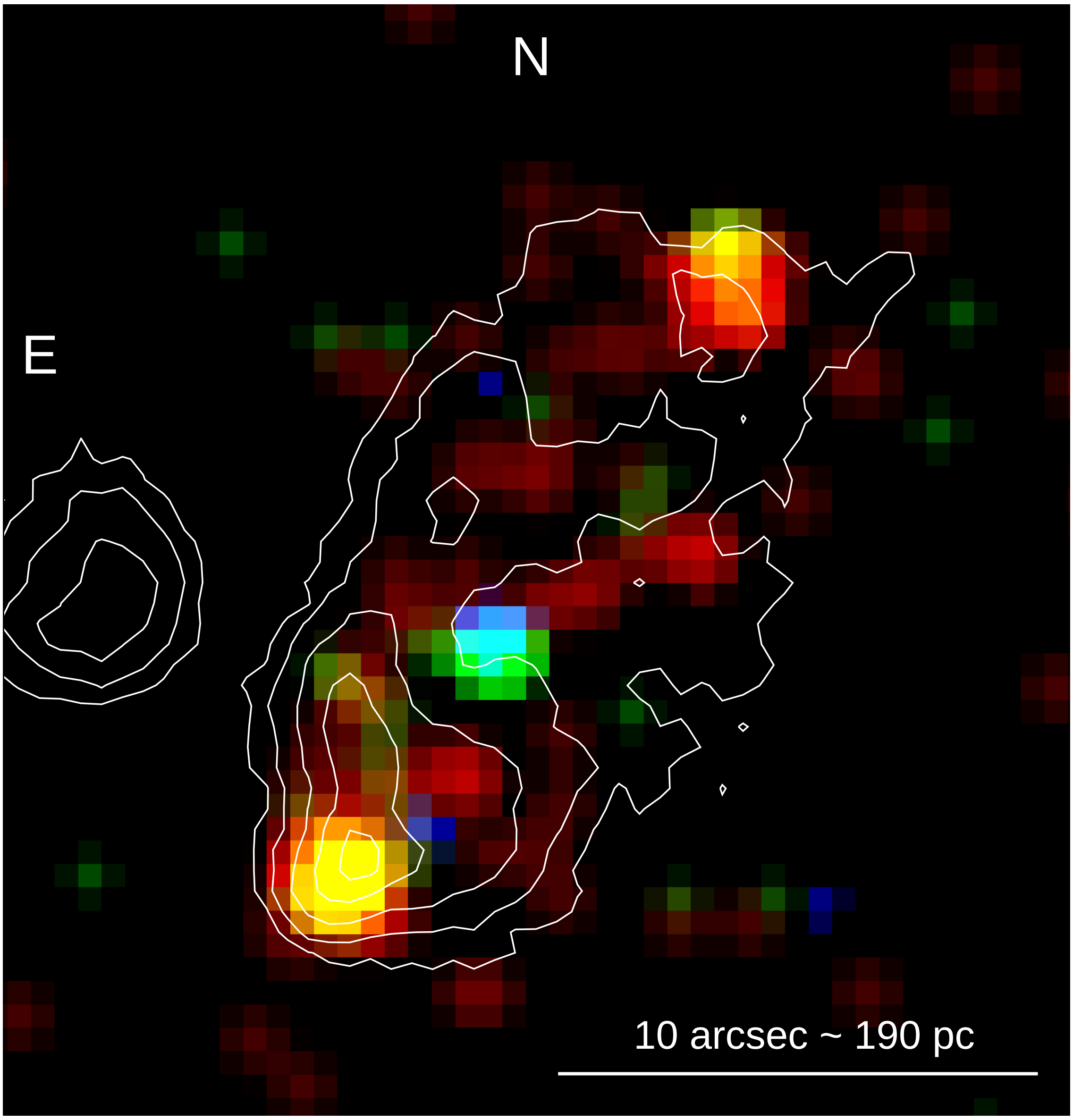
N
E
10 arcsec ~ 190 pc

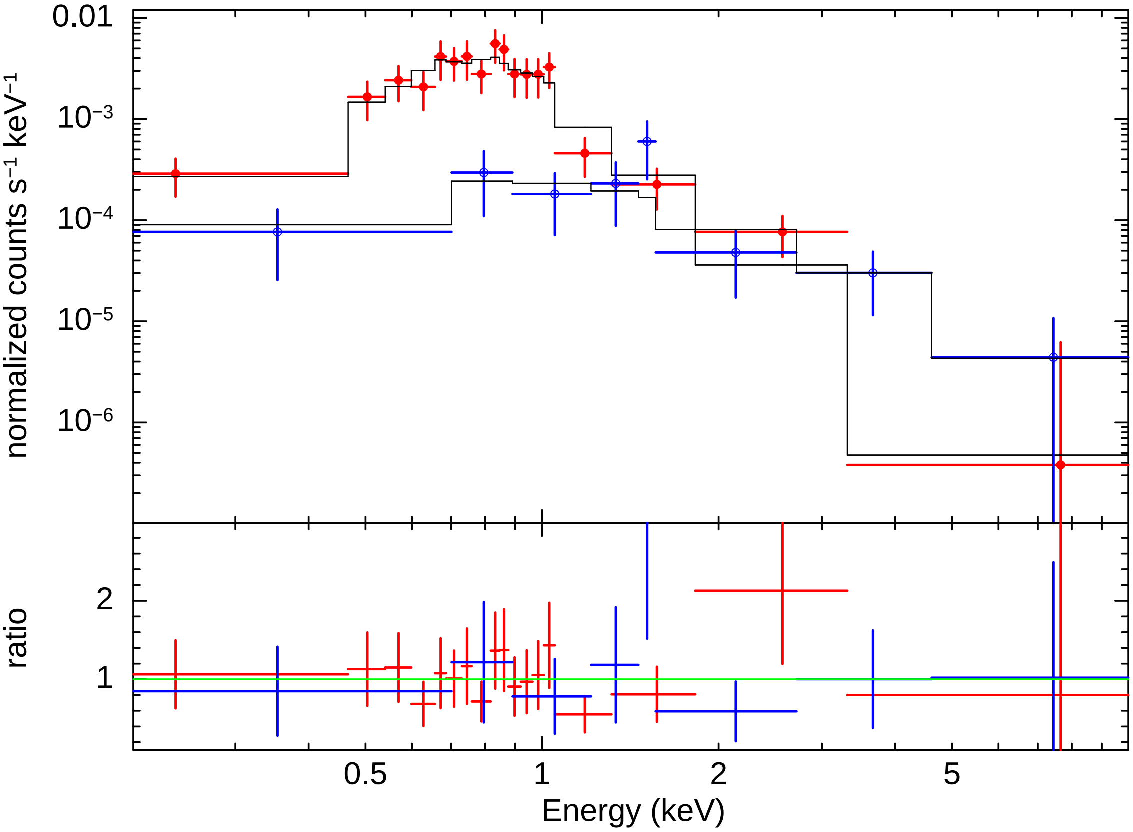
0.01
10^{-3}
10^{-4}
10^{-5}
10^{-6}
normalized counts s^{-1} keV^{-1}
ratio
2
1
0.5
1
2
5
Energy (keV)

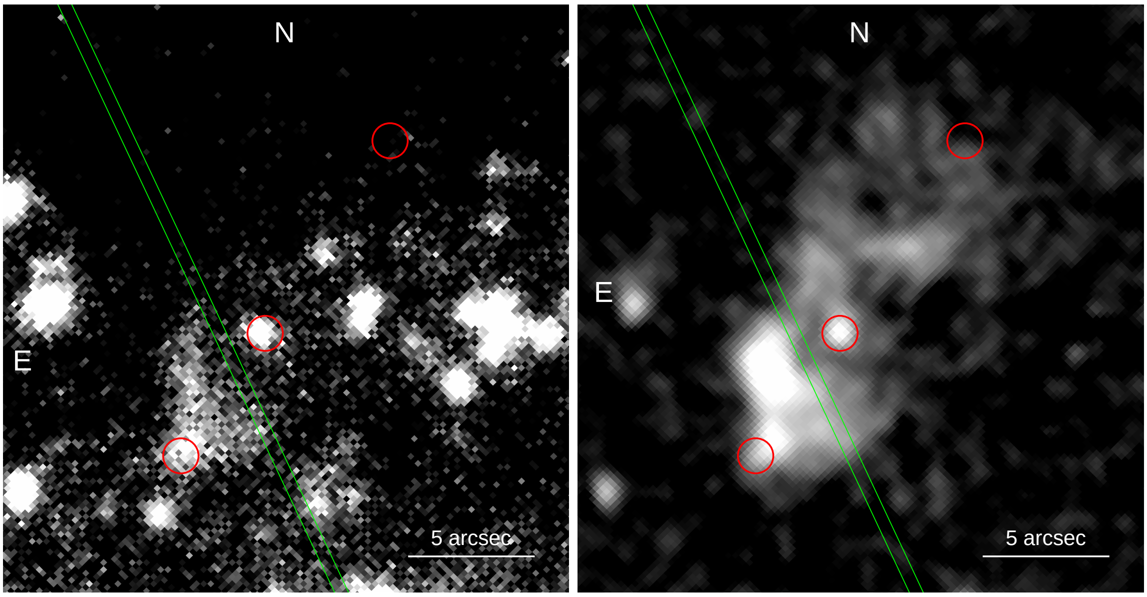
N
E
5 arcsec
N
E
5 arcsec

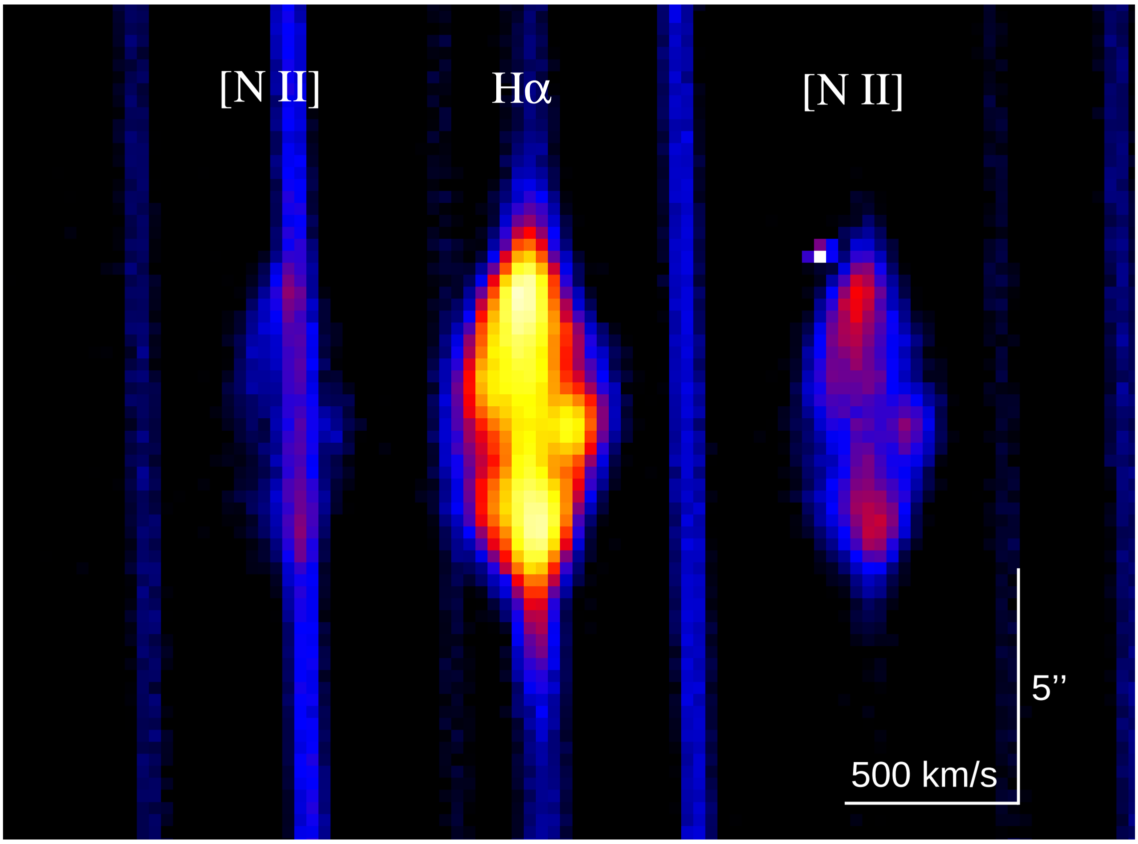
[N II]
Hα
[N II]
5''
500 km/s